A STUDY OF THERMAL EFFECTS IN A PROTON EXCHANGE MEMBRANE FUEL CELL WITH A TWO-FLUID MODEL

Berning, T.
Department of Energy Technology,
Aalborg University,
9020 Aalborg,
Denmark,
E-mail: tbe@et.aau.dk

ABSTRACT

Proton exchange membrane fuel cells (PEMFC) are considered a key future technology for both automotive and stationary applications. At high current densities the performance curve of a PEMFC deviates from the linear region where the cell losses are dominated by the ohmic resistance, and the cell performance deteriorates rapidly. This phenomenon has often been assigned to mass transport losses because conventional fuel cells rely on diffusion of the reactants to reach the catalyst layers. This study will investigate the role of thermal properties on expected cell performance in general and on the membrane hydration level in particular. The two key thermal properties that have been investigated in detail in this study are the thermal conductivity of the porous gas diffusion layers k, and the thermal contact resistance between the gas diffusion layer and the bipolar plates. At a high current density of 1.0 A/cm^2 the difference in the average predicted membrane hydration level varies from $\lambda = 8.92$ for the best case to a value down to $\lambda = 7.73$ for the worst case. The difference in the predicted maximum temperature in the cell is more severe. The main conclusion is that it is highly recommended to use dense gas diffusion media with lower porosity but higher thermal conductivity when employing the interdigitated flow field.

INTRODUCTION

Proton exchange membrane fuel cells are currently being commercialized by several automotive manufacturers including Toyota and Hyundai who are both starting to offer fuel cell vehicles to customers. The fuel cells used to power vehicles are low-temperature proton exchange membrane fuel cells that operate below 100 ℃, and they combine internally hydrogen with oxygen from air to produce electricity, the only by-products being water and waste heat. The detailed reactions are:

$$\begin{aligned} &Anode: 2H_2 \Rightarrow 4H^+ + 4e^- \\ &Cathode: \mathrm{O}_2 + 4H^+ + 4e^- \Rightarrow 2H_2O \\ &Combined: 2H_2 + O_2 \Rightarrow 2H_2O \end{aligned} \qquad (1)$$

The protons created in the anode side reaction migrate through a proton conducting membrane, and the electrons pass through an external electrical circle and provide electrical work. The driving potential is the cell potential. Water is created at the cathode, but when both reactant gases enter the cell dry a certain fraction of it crosses through the membrane towards the anode and humidifies the anode gas and the membrane. It is important to keep the membrane hydrated because its proton conductivity depends strongly on its water content [1].

A schematic of a PEMFC is shown in Figure 1. The flow channels are typically up to 20 *cm* long and have a height and width in the order of 1 *mm*, usually a bit smaller. The bipolar plates are often made out of graphite or stainless steel for easier mass production. The gas diffusion layer (GDL) is usually a porous carbon fiber paper that allows for gas diffusion and convection and electron conduction. The catalyst layers contain platinum nanoparticles and are around 10 *microns* thick. The polymer electrolyte membrane in the center of the cell is around 20 to 50 *microns* thick. A typical material is DuPont's Nafion®. A single cell has a maximum electrical potential below 1 *V* and is operated at a maximum current density below 2 A/cm^2. Therefore, around 100 single cells or more have to be combined in a fuel cell stack to obtain sufficient electrical power for automotive purposes.

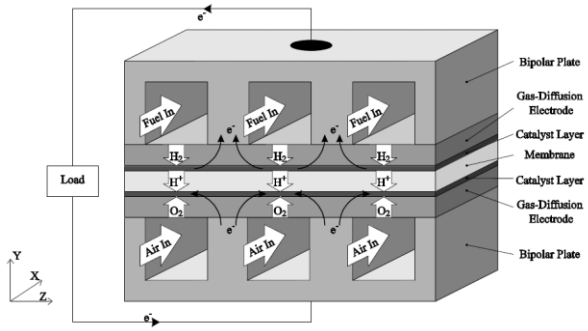

Figure 1 Schematic of a PEMFC [2].

While PEMFC's are currently being commercialized, it is still important to obtain more fundamental knowledge of the thermal effects in the fuel cell, particularly at high current densities where the typical performance curve starts to deviate from the linear behavior. This operating regime is usually called the mass transport limited regime and the maximum current that can be drawn from a fuel cell is in fuel cell textbooks often determined by the diffusion limitation of oxygen (e.g. [3]). Figure 2 compares the performance for a fuel cell that has an ohmic resistance similar to a commercial stack with and without mass transport losses [4].

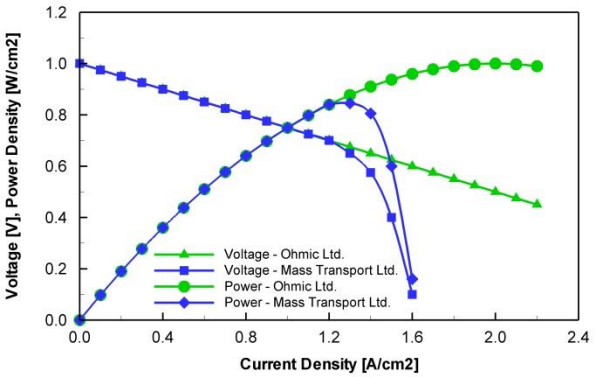

Figure 2 Fuel cell performance for a typical ohmic resistance with and without mass transport limitations.

Without mass transport losses the achievable power density is substantially higher. It can also be seen that even in this case it makes no sense to operate that fuel cell beyond a current density of 2.0 A/cm^2 as from here the power density starts to decrease. In the case with mass transport limitations the maximum current drawn should not exceed around 1.2 A/cm^2. Clearly, higher current density operation is generally desired as it would reduce the overall cell area that is needed and thereby save cost. The condition is that the power density also increases. In order to further increase the power density it would be necessary to reduce the so-called activation overpotential that is associated with the electro-chemical reactions or further reduce the ohmic resistance of the cell, ideally both. The activation overpotential might be decreased by increasing the catalyst loading or increasing the operating temperature. The ohmic loss is attributed to the electrolyte membrane and the contact resistances between the various layers of the cell.

Figure 3 shows the calculated amounts of waste heat for the cases with and without mass transport limitations.

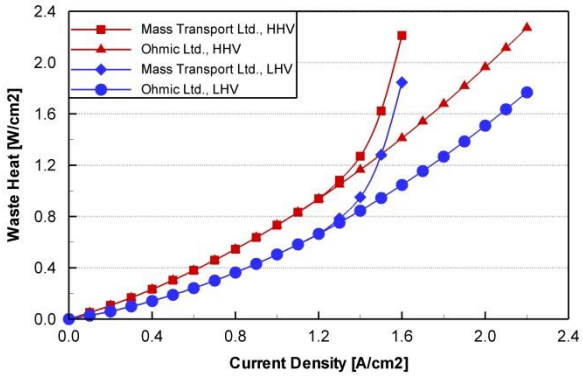

Figure 3 Calculated amount of waste heat based on the cell performance from Figure 2.

If the reaction enthalpy ΔH of reaction (1) could be converted into electricity the theoretical maximum voltage would be 1.482 V based on the higher heating value and 1.254 V based on the lower heating value [4]. The calculated amount of waste heat is then either of these two values minus the actual cell potential as shown in Figure 2, depending on the thermodynamic phase in which the product water leaves the cell. While the amount of waste heat that incurs in a fuel cell has to be calculated from the reaction enthalpy, the theoretical maximum cell voltage can be calculated out of Gibbs free energy ΔG, and it is 1.23 V at room temperature and 1.184 V at the typical operating temperature of 80 $^{\circ}C$ [4]. Figure 3 shows clearly the advantage of having the product water leave the cell in the gas phase and the necessity of avoiding to operate in the mass transport limited regime.

One possibility to avoid the mass transfer regime altogether is to employ interdigitated flow fields (IFF's), first described by Nguyen [5]. These flow fields promote convection of the reactants towards the catalyst layers instead of relying on diffusion that requires a concentration gradient from the flow channels to the catalyst layers. In essence the interdigitated flow field has dead-ended inlet section so that the reactant gas is forced through the porous gas diffusion layer (GDL) (sometimes combined with a micro-porous layer – MPL) towards the outlet section. A schematic of an IFF is shown in Figure 4.

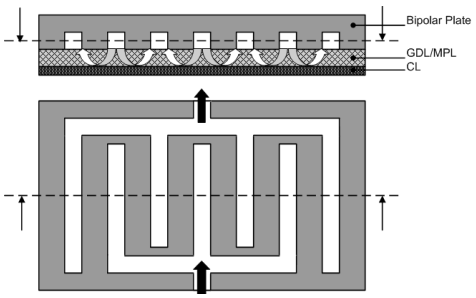

Figure 4 Schematic of an interdigitated flow field [6].

While it is frequently argued that the IFF leads to too high pressure drops, our group has shown that an important advantage of the IFF lies in the possibility of operating at low stoichiometric flow ratios which leads to a substantially reduced compressor work [6]. With our computational model we have recently shown that stoichiometric flow ratios as low as ξ_{Ca} = 1.1 at the cathode and ξ_{An} = 1.03 at the anode are possible [7]. The latter is very important as this would mean that it is not required anymore to recirculate at the anode outlet which greatly reduces the cost and complexity of a fuel cell system. Our group was also the first to show that fuel cell operation on completely dry inlet gases is possible even at high current densities when a so-called water uptake layer is added at the cathode catalyst layer [8].

In order to further increase the fuel cell efficiency, it is desired to

a) reduce the ohmic losses, and
b) increase the cell temperature.

The main sources for ohmic losses are membrane dehydration and the contact resistance between the bipolar plates and the porous gas diffusion layer. The proton conductivity of the electrolyte membrane is a strong function of its water content, and in general a higher water content leads to a higher proton conductivity and is thus preferred [1]. However, a fully hydrated membrane will come at the cost of excessive water inside the fuel cell, and in particular the blocking of channels by liquid water should be avoided as it will cause

reactant mal-distribution which is particularly detrimental at low stoichiometries. The membrane loss increases when the membrane becomes dehydrated, and therefore it has been suggested to operate the fuel cell at temperatures close to the respective dew point temperatures of the anode and cathode outlet gases [9]. These dew point temperatures only depend on the back pressure, the stoichiometric flow ratios and the fuel cell water balance [9]. It was previously shown how dew point diagrams can be constructed and used to optimize fuel cell operating conditions in such a way that the outlet gas streams are saturated with water vapour at both anode and cathode while the inlet gas streams were completely dry (0% relative humidity) [10]. Examples for such operating conditions are listed in Table 1. Provided that the fuel cell water balance, characterized by the effective drag coefficient r_d, assumes a value of r_d = -0.014 both outlet gases will be saturated with water vapour which means that all product water leaves the cell in the gas phase. The definition of the effective drag coefficient is here:

$$r_d = \frac{\dot{n}_{H_2O}^{an,out} - \dot{n}_{H_2O}^{an,in}}{I/F} \qquad (2)$$

i.e. it is the difference in the molar water vapour stream between anode outlet and anode inlet which has been non-dimensionalized by the total fuel cell current I and Faraday's constant F (96485 *C/mole*). Clearly, when the fuel cell is operated on dry hydrogen the effective drag can only be negative.

Table 1 Summary of operating conditions found with the help of dew point diagrams.

Property	Anode	Cathode
Inlet temperature [°C]	80	85
Stoichiometric flow ratio [-]	1.03	1.1
Inlet relative humidity [%]	0.0	0.0
Outlet pressure [atm]	1.2	1.5

A higher operating temperature is expected to lead to an improved cell performance because it should reduce the activation overpotential associated to the chemical reactions. However, in order to increase the general fuel cell operating temperature, local peak temperatures which may lead to membrane punctuation have to be reduced. These are usually found in the fuel cell membrane or the cathode catalyst layer, and it can exceed the average cell temperature by 5 to 15 ℃, depending on the current density distribution and effectiveness of waste heat removal.

It is the goal of the current study to investigate the effect of thermal properties of the fuel cell on the predicted membrane hydration level and the predicted peak temperatures with a state-of-the-art computational model of a PEMFC employing computational fluid dynamics. Key thermal properties are the thermal conductivity of the porous media inside the fuel cell and the thermal contact resistance between these porous media and the fuel cell bipolar plate. Starting from a base case, different values for each of these properties will be used in our computational model at two current densities. The assumed amount of waste heat is the same for the same current density which demonstrates one great advantage of using a computational model to investigate different *What if?* scenarios.

MODEL DESCRIPTION

The fuel cell model used in this study has been extensively described in previous publications [6,8,11]. It is based on the formerly commercial software package CFX-4 (*ANSYS Inc.*), a classical *I, J, K*- structured, multi-block CFD code. Salient features of the model are:

- Three-dimensional geometry that includes anode and cathode flow channels, bipolar plates, gas diffusion layers, micro-porous layers, catalyst layers and the polymer electrolyte membrane.
- Capability of modeling either conventional straight channel flow fields or interdigitated flow fields in co-or counter-flow mode.
- Multi-phase flow of water is described using the multi-fluid approach, *i.e.* one set of conservation equation is solved for each thermodynamic phase considered which is the most rigorous treatment of multi-phase flow.
- Capillary action of liquid water through the porous media is described by the so-called Leverett function [12]. The fraction of hydrophilic pores inside porous media is accounted for by the irreducible saturation.
- Non-equilibrium phase-change of water is accounted for where the driving force is the deviation from full saturation. This includes the area of the liquid/gas interface.
- The model is non-isothermal. Thermal contact resistances between different solid layers (GDL and BP) are accounted for.
- Cathode side includes species equation for oxygen and water (liquid and gas) anode side includes hydrogen and water (liquid and gas).
- Three-dimensional model for water transport through polymer electrolyte membrane considering non-equilibrium absorption/desorption, electro-osmotic drag, diffusion and hydraulic permeation through the open pores.
- Simplified electro-chemistry that assumes a three-dimensional current density inside the CL's to calculate local sink and source terms of reactants inside catalyst layers; pre-specified total current density corresponds to total amount of oxygen and hydrogen consumed and water and waste heat produced.

As is shown in Figure 5, the fact that an *I, J, K*- structured mesh is used allows for the computational disconnection of the different physical domains which is very convenient for modeling purposes.

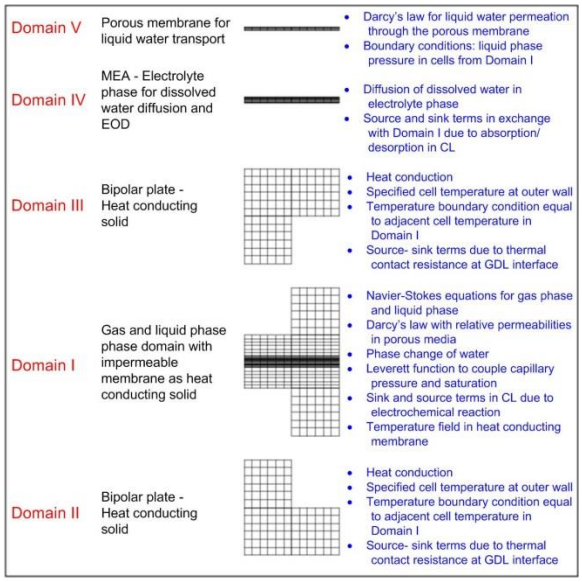

Figure 5 General set-up of our multi-phase PEMFC model showing the numerical grid in a 2D cut and the different computational domains.

In general, *Domain I* is the main computational domain where the multi-phase flow and species equations are solved. *Domains II and III* represent the bipolar plates where we are currently only interested in the heat transfer equation. A temperature boundary condition is imposed at the outer surfaces where the coolant would be, and the cells bordering to the inner surfaces communicate with the corresponding neighboring cells of *Domain I*. *Domain IV* is a copy of the membrane and the CL's of *Domain I*. This sandwich is also called the membrane-electrode-assembly (MEA). In *Domain IV* we are only interested in calculating the transport of water that is dissolved in the electrolyte phase. Simply put, in order for the water to cross from cathode to anode in *Domain I*, it has to absorb from the cathode CL of *Domain I* to the corresponding control volume (CV) of *Domain IV*, diffuse through the electrolyte phase of *Domain IV*, and then desorb from the anode CL in *Domain IV* to the corresponding CV in *Domain I*. These absorption and desorption terms are accounted for as sink and source terms for the water transport equation in the respective domains. This appears complex, but it allows for a clean implementation of the water cross-over and is numerically very robust.

When the interdigitated flow field is to be modeled the computational domains have to include two channels each, one dead-ended inlet section and one outlet section. Figure 6 shows the numerical grid for the main computational domain (*Domain I*) and a calculated velocity field to illustrate the interdigitated flow field. The general flow arrangement is counter-flow which means that the hydrogen at the anode and the air at the cathode enter at different ends of the cell. This is owing to the effect that the anode and cathode outlet temperatures should be different according to dew point diagrams.

The channel length in this case is 5 *cm*, but it has been found that increasing the channel length to 10 *cm* or longer does not qualitatively affect the results. Typical fuel cells have channel length of 10-20 *cm*.

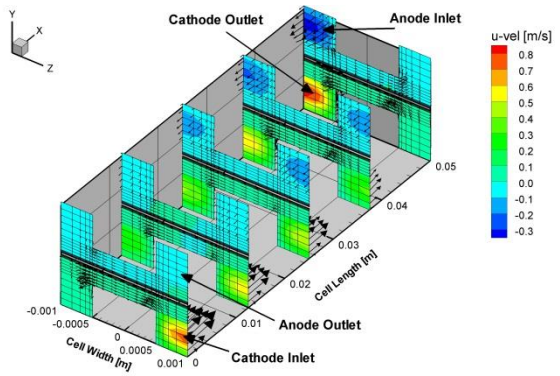

Figure 6 General flow configuration and numerical grid of the interdigitated flow field [13].

MODELING STUDY

The operating conditions investigated correspond to the ones applied in previous studies, and they are summarized in Table 1. In a previously published study the effect of the channel width and the land area width on the membrane hydration level was investigated, and it was found that the finest channel width leads to the best membrane hydration. This could be attributed to the fact that peak temperatures occur under mid-channel. Hence, the current study employs a land and channel width of 0.5 *mm* each.

In the current study the two main properties of interest are the thermal conductivity k of the porous media that are located between the flow channels and the catalyst layer as well as the contact resistance R between the gas diffusion layer and the bipolar plate. Table 2 lists the *base case* conditions.

Table 2 Key material parameters investigated in this study and their corresponding base case values

Property	Symbol	Unit	Value
GDL thermal conductivity	k_{GDL}	W/mK	1.0
MPL thermal conductivity	k_{MPL}	W/mK	1.0
GDL/BP contact resistance	R	m^2K/W	2.0×10^{-5}

Karimi *et al.* [14] have determined the thermal conductivity to be in the range from 0.26 *W/m-K* up to 0.70 *W/m-K* under compression. The value for the thermal contact resistance was measured by that group to be between 0.6 and 2.4×10^{-4} m^2*-K/W*. These values depend on the contact pressure applied to the stack and the treatment of the GDL.

In this study the amount of waste heat that is produced in the fuel cell increases linearly with the current density. For the base case the potential loss was estimated to be 500 *mV* at the cathode and 50 *mV* at the anode. While especially the former value may appear quite high to the expert, it has to be stressed that these two terms are currently the only losses that are accounted for in the model and hence should roughly account for the difference in the cell potential of 1.28 *V* that can be calculated out of the reaction enthalpy and the operating cell

potential that typically ranges from 600 mV – 800 mV. If all product water would leave the cell in the liquid phase the corresponding cell potential would be 1.45 V. The above losses have been assumed independent of the current density. This is in contrast to the fuel cell performance curve as shown in Figure 2 which indicates that the potential loss increases with current density. However, it has been pointed out above that the overall amount of waste heat is the potential loss compared to 1.28 V multiplied with the current density of the fuel cell. Therefore, in the current study the amount of waste heat increases strongly with current density – although not as strongly as would be realistic. For this analysis it is deemed important that the amount of waste heat increases with current density, and that the same amount of waste heat is produced for a given current density. Variation of the thermal properties will then indicated, how strongly the membrane hydration level and the peak temperature in the cell will be affected.

RESULTS AND DISCUSSION

Base case results

First the base case results will be shown for two different current densities, 0.4 A/cm^2 and 1.0 A/cm^2. The membrane water content gives a good indication of the proton conductivity of the membrane, and the calculated water distribution for the different current densities is shown in Figure 7.

The maximum value for a membrane equilibrated with water vapour is $\lambda \approx 14$. What can be observed in Figure 7 is that an increase in the current density leads to more severe membrane dry-out especially towards the cathode outlet/anode inlet. It should be kept in mind that this is the cold end of the fuel cell because the coolant is assumed to run in co-flow to the anode gas streams (see also Table 1). In that light is appears surprising that the cold end is also the dry end of the cell, but so far all calculations have indicated the same trend. A potential remedy was proposed earlier in suggesting to place the expensive platinum catalyst only at the first 80 % of the cell length and hence utilize the membrane where it is both hot and wet. This may or may not be easily verified by building a fuel cell with an MEA that contains only catalyst in select regions and measure the performance. Overall it can be stated that an increase in current density is predicted to result in a decrease in the membrane hydration level which consequently will lead to an increase in the ohmic loss and a deviation from the linear behaviour of the cell potential at elevated current densities.

While frequently the argument is heard that at higher current densities, more water is being produced that will better hydrate the membrane, this argument is flawed: when the stoichiometric flow ratio is kept constant the anode and cathode dew point temperatures remain unchanged, so that if the water balance is similar both outlet gas streams will be at the same level of saturation and hence the same wetness. On the other side, an increase in current density invariably leads to an increase in the amount of waste heat produced and that can result in membrane dehydration. An important question is thus, how effectively this waste heat is removed from the cell.

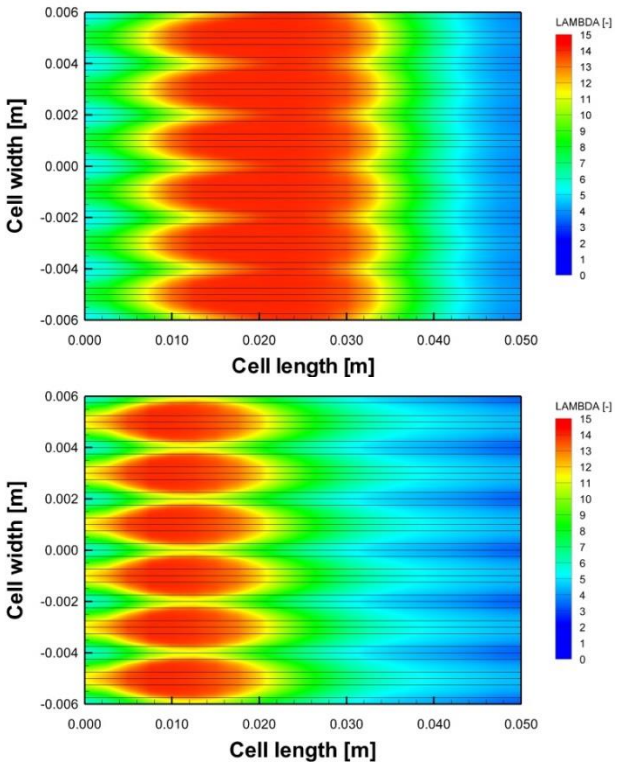

Figure 7 Predicted membrane water distribution for the base case at 0.4 A/cm^2 (upper) and 1.0 A/cm^2 current density (lower). The cathode flow direction is from left to right and anode from right to left. The single computational domain was 1.0 mm wide and the results have been mirrored several times for better visualization.

A common source for the above misconception is that in numerous experimental studies the gas flow rates were kept constant irrespective of the current densities. This is a fatal error that leads to a decrease in the stoichiometric flow ratios with increasing current densities and therefore the cell may become wetter. The stoichiometric flow ratio is a key parameter in fuel cell operation and comparable results can only be obtained when keeping this parameter constant. Most certainly, automotive fuel cells operate at a constant anode and cathode stoichiometry. For different applications however, a blower may be used at the cathode side at constant power and thereby the effective stoichiometry may not be constant during operation, after all.

Variation of the porous media thermal conductivity

The first parameter that has been studied is the thermal conductivity of the porous media, and the value for both k_{GDL} and k_{MPL} has been changed to 0.5 $W/m\text{-}K$ *and* 2.0 $W/m\text{-}K$, respectively. The resulting effect on the predicted membrane hydration level is particularly obvious at the elevated current density of 1.0 A/cm^2, shown in Figure 9. The average membrane hydration levels are λ_{ave} = 7.80 and λ_{ave} = 8.88, respectively.

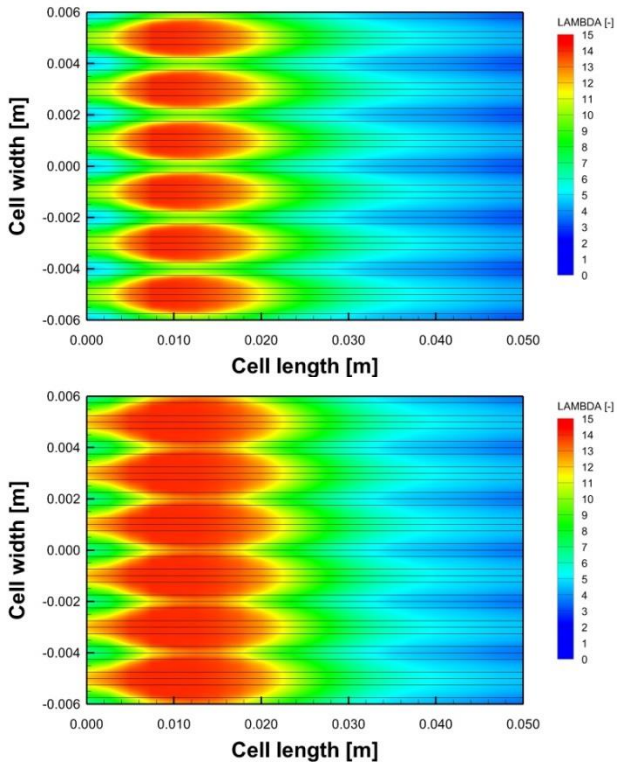

Figure 8 Predicted membrane water distribution at 1.0 *A/cm²* for a porous media thermal conductivity of 0.5 *W/m-K* (upper) and 2.0 *W/m-K* (lower).

The resulting peak temperatures in the cell are 366.28 *K* and 360.82 *K,* respectively, which shows the very strong effect that the thermal conductivity has on the general thermal management. These temperatures have to be put into relation to the maximum temperature that has been applied as a boundary condition at the outer boundaries of the bipolar plates where the coolant would be located. According to Table 1, this temperature has been specified to 85 ℃ (358.15 K) at the anode outlet so the predicted temperature increase ranges from less than 3 *K* to more than 8 *K* depending on the thermal conductivity of the GDL. Obviously, it is highly desirable to choose a GDL with as high a thermal conductivity as possible. It is also clear that the GDL thickness plays an important role in thermal management as well (not investigated here), and from a thermal perspective it should be as thin as possible. On the other hand, Yablecki and Bazylak have found that the thermal conductivity of thin GDL materials is lower than for thick GDL materials, which was attributed to boundary effects [15] where a thinning out of the fibers occur. These authors have found that the GDL conductivity in the core of the materials may be as high as 1.6 *W/m-K*.

Variation of the thermal contact resistance

The other parameter of interest that has been studied here is the thermal contact resistance at the interface between the GDL and the bipolar plates. The base case parameter of R_{th} = 2.0×10^{-5} m^2-*K/W* has been changed to 1.0×10^{-5} m^2-*K/W* and 4.0×10^{-5} m^2-*K/W,* respectively, while keeping the thermal conductivity at its base case value of 1.0 *W/mK*. The finding was that the thermal contact resistance only has a weak influence on the results. The calculated average membrane water content λ_{ave} and the resulting peak temperature T_{max} at a current density of 1.0 *A/cm²* are summarized in Table 4. The "worst case" with the lowest thermal conductivity paired with the highest contact resistance is Case 5 and the "best case" is Case 6. The difference in the predicted maximum temperature was nearly 6 K. Considering the above reasoning that in general it is desirable to increase the fuel cell operating temperature while avoiding too high peak temperatures, a difference of 6 K is very substantial: by optimized thermal management one may increase the general fuel cell operating temperature by as much as 5 K and thereby expect a reduction in activation losses due to reaction kinetics (hence an increase in cell performance or a reduction in Pt loading). Moreover, a higher operating temperature will lead to a decrease in the automotive radiator. The differences in the predicted membrane hydration level do not appear as drastic, but it must be kept in mind that a drier membrane induces higher losses and therefore a higher ohmic heating term: the waste heat production would increase and thereby the effect is compounded.

Table 4 Case study and the predicted average membrane hydration and peak temperature at 1.0 *A/cm²*.

Case	k_{GDL} [W/mK]	R_{th} [m^2-K/W]	λ_{ave} [-]	T_{max} [K]
Base Case	1.0	2.0×10^{-5}	8.32	362.74
Case 1	0.5	2.0×10^{-5}	7.76	366.38
Case 2	2.0	2.0×10^{-5}	8.88	360.82
Case 3	1.0	4.0×10^{-5}	8.35	363.02
Case 4	1.0	1.0×10^{-5}	8.42	362.64
Case 5	0.5	4.0×10^{-5}	7.73	366.60
Case 6	2.0	1.0×10^{-5}	8.92	360.70

CONCLUSION

A numerical study has investigated thermal effects in a proton exchange membrane fuel cell in order to better understand the phenomenon of membrane dry-out. The two key material parameters that have been studied were the thermal conductivity of the porous layers and the thermal contact resistance between the porous media and the bipolar plates. Using constant operating conditions the membrane was predicted to increasingly dry-out due to the increasing waste heat production. Therefore, the fuel cell polarization curve will deviate from its ohmic region so that what is frequently considered the mass transport limited regime of a polarization curve is in part caused by increased ohmic losses.

For thermal management, it is desirable to use GDL with as high a thermal conductivity as possible paired with a low thermal contact resistance. This may also include denser GDL materials with lower porosity. While highly porous materials are required when using the conventional flow field to enhance mass transport, in case of the interdigitated flow field this poses no problem, and denser GDL/MPL should be employed.

ACKNOWLEDGEMENTS

This project has been sponsored by EUDP, J.nr. 64012-0117 and by PSO under the ForskEL program, Project nr.2013-1-12041.

REFERENCES

[1] T.E. Springer, T.A. Zawodzinski, S. Gottesfeld. Polymer Electrolyte Fuel Cell Model, J. Electrochem. Soc. 138 (1991) 2334-2342.

[2] T. Berning, Three-dimensional computational analysis of transport phenomena in a PEM fuel cell, PhD Dissertation, University of Victoria, (2002).

[3] R. O'Hayre, S. Cha, W. Colella, F. B. Prinz, Fuel Cell Fundamentals, Wiley 2006.

[4] F. Barbir, PEM Fuel Cells - Theory and Practice, 2012.

[5] T.V. Nguyen. A gas distributor design for proton-exchange-membrane fuel cells, J. Electrochem. Soc. 143 (1996) 103-105.

[6] T. Berning, M. Odgaard, S. K. Kær. A study of multi-phase flow through the cathode side of an interdigitated flow field using a multi-fluid model, J. Power Sources. 195 (2010) 4842-4852.

[7] T. Berning, S. K. Kær. Low stoichiometry operation of a proton-exchange membrane fuel cell employing the interdigitated fuel cell – a modeling study, International Journal of Hydrogen Energy. 37 (2012) 8477-8489.

[8] T. Berning, M. Odgaard, S. K. Kær. Water balance simulations of a polymer-electrolyte membrane fuel cell using a two-fluid model, J. Power Sources. 196 (2011) 6305-6317.

[9] T. Berning. The dew point temperature as a criterion for optimizing operating conditions of proton exchange membrane fuel cells, J. Power Sources. 37 (2012) 10265-10275.

[10] T. Berning. Employing dew point diagrams to optimize PEMFC operating conditions, ECS Transactions. 50 (2012) 557-568.

[11] T. Berning, M. Odgaard, S. K. Kær. A computational analysis of multi-phase flow through the porous media of a PEMFC cathode using the multi-fluid approach, J. Electrochem. Soc. 156 (2009) B1301.

[12] M. C. Leverett. Capillary behavior in porous solids, Trans. AIME. 142 (1976) 152.

[13] T. Berning, MULTIPHASE SIMULATIONS AND DESIGN OF VALIDATION EXPERIMENTS FOR PROTON EXCHANGE MEMBRANE FUEL CELLS, Proc. ASME. 55560; Volume 1C (2013).

[14] G. Karimi, X. Li, P. Teertstra. Measurement of through-plane effective thermal conductivity and contact resistance in PEM fuel cell diffusion media, Electrochimica Acta. 55 (2010) 1619-1625.

[15] J. Yablecki, A. Bazylak. Determining the effective thermal conductivity of compressed PEMFC GDLs through thermal resistance modelling, Journal of Power Sources. 217 (2012) 470-478.